Radiation Leakage and the Precision of Characterizing Nuclear Material Using Calorimetric Assay – 19233

Wojciech R. Kubinski[*], Cedric Carasco[**], Daniel Kikola[*], Christophe Mathonat[***],
Bart Rogiers[****], Dariusz Tefelski[*], Holger Tietze-Jaensch[*****]

[*]Politechnika Warszawska, Plac Politechniki 1, Warszawa 00 661, Poland
[**]CEA/DEN/DTN Cadarache, F-13108 Saint-Paul-Lez-Durance, France
[***]KEP Nuclear, 453 Chemin Vieux de Chusclan, Bagnols-sur-Cèze 30200, France
[****]SCK•CEN, Boretang 200, 2400 Mol, Belgium
[*****]Forschungszentrum Jülich, Wilhelm Johnen Strasse, Jülich 52428, Germany

ABSTRACT

For measuring a waste drum containing multi-nuclide radioactive material calorimetric assay is often combined with gamma ray and neutron measurements [1, 2]. To reduce the methodological uncertainties of the inventory determination in a multi-nuclide matrix, the escaping radiation must be quantized as much as the encapsulated gamma-rays and α-, β-, n- particles depositing radiological heat inside the drum. To differentiate the possible variety of heat sources in a radioactive waste drum, Monte Carlo simulations are utilized resembling the waste drum and the calorimeter in both, their geometries as well as the material compositions.

MCNP6-based numerical imaging of the Large Volume Calorimeter (LVC) designed by KEP Nuclear*** (France) allows simulating various scenarios for different particles types, energies and source locations to accompany and support the interpretation of calorimetric KEP-LVC measurements anticipated within the CHANCE project [3, 4, 5]. For the analyses, the particle flux and energy deposition in each layer of the calorimeter are displayed. The results yield that a significant part of the emitted radiation leaves the system and does not contribute to the heat deposited inside the drum.

As an example, the particle flux study of a 200L mock-up drum placed inside the KEP-LVC calorimeter is discussed. A tally 4 with mesh option for both gamma and neutrons up to 5MeV simulates the mean flux in each cell and for various source location and source distribution patterns. The expected energy deposition is cumulated for each layer, and over the whole energy range it reveals that actually a small but well known fraction of particles escapes the LVC calorimeter. This makes it a very suitable apparatus for the anticipated experiments on large and heterogeneous waste drums. The results suggest that the most interesting cases would be polyethylene, bitumen and concrete matrices [3, 5]. However, it must be kept in mind that the high-energy part of the gamma and neutron radiation flux can reach the reference chamber of the calorimeter and deposit some energy there, which may compromise the calibration and cause double-bias.

The simulations showed that, depending on source location and power, neutron and high-energy gamma radiation leakage can influence the heat measurements differently. In general, part of the simulation results suggest that for waste drums with a high emission rate the accuracy of calorimetric assay can be decreased due to radiation escape.

INTRODUCTION

Calorimetry is a non-destructive method of quantitative measuring the heat emission to determine the masses or activities of nuclear material hidden inside nuclear waste compounds. Heat-flow calorimeters are in common use for measuring thermal powers over a wide range of 0.5mW (equivalent to 0.2g of low-burnup plutonium) up to 1kW and for samples of various sizes of about a few cm³ up to large waste drums of 60cm wide and 100cm long [1].

For measuring a multi-nuclide drum calorimetric assay is often combined with gamma ray and neutron measurements [1, 2]. Calorimetric determination of tritium and plutonium activities or masses has become common practice. However, the determination of beta-emitters (e.g. Sr/Y-90) or shielded sources inside a concrete filled waste compound is yet challenging for the comprehensive nuclide characterization of large heterogeneous waste drums.

Ideally, non-destructive assay (NDA) of radioactive waste drums should be able to provide information concerning the type, amount and distribution of radionuclides, as well as information of the physical and chemical state of the waste. A vast amount of literature on the characterization of nuclear inventories already exists, and also many studies compare NDA techniques for radioactive waste characterization [6, 7, 8, 9, 10]. In the context of the CHANCE work-package 3 [3, 4], the ESARDA report [11] is particularly relevant since it performs a quantitative comparison of the techniques in term of Minimum Detectable Mass (MDM).

A benchmark of calorimeters and standard NDA methods for the characterization of large volume waste drums [5] facilitates an evaluation that is performed through a study of the neutron and gamma ray signals that can escape various 200L waste drum matrices with different source configurations, and through a comparison with the published plutonium and uranium Minimum Detectable Masses (MDM) of existing systems.

Of course, basic and fast NDA methods would measure the gamma dose rate of a waste package. The interpretation of a dose measurement for NDA requires a very good knowledge of the nuclide vector associated with the particular waste package, as well as its physical properties. Therefore, dose rate measurement provides incomprehensive information concerning NDA characterization of the nuclear content. When gamma- and/or neutron assay of radwaste containers provide inadequate results, because of the container size, heterogeneity of the material matrix or simply because of buried difficult-to-measure (DTM) nuclides, then calorimetry proves a viable though ancillary tool to complement and supplement the task of a comprehensive NDA characterization.

The decisive goal is to establish a significantly reduced MDM-level for DTM-nuclides, e.g. buried sealed sources or beta-emitters with no or a weak gamma signal, such as the declarable Sr-90 nuclide beta-decaying into Y-90 with practically no detectable gamma footprint.

CALORIMETRY FOR NUCLEAR ASSAY AND APPLICATION

The measurement of the heat generated by a nuclear sample through calorimetry combined with a measurement of the nuclear isotopic mass ratios of the samples by another Non Destructive Assay (NDA) technique (e.g. High Resolution Gamma Spectrometry) provides a convenient and accurate measure of the total radioactive mass of the sample. Currently, calorimetry represents the most accurate and precise NDA measurement of the masses of nuclear materials, if the isotopic vector is known. Therefore, it has a great potential for the characterization of radioactive nuclear wastes and for safeguards purposes.

Calorimetry measurement technology encompasses the following advantages compared to other NDA techniques [2, 5]:

- Very high precision, ranging from ~0.5% for low power items (≤0.2W) to ~0.1% for items dissipating more than 1W. If the isotopic composition of the item can be accurately determined with another NDA technique, the precision of the calorimetric measurement is comparable to chemical analysis, making calorimetry the most precise NDA technique for nuclear materials.
- The calorimetric analysis involves the entire mass, so that the result is not the extrapolation from a limited specimen. Thanks to this, the result is independent of nuclear material distribution within the sample. This feature is very important when the distribution of the sample is not known in advance and it cannot be extrapolated. Note that gamma or neutron radiation, dependent on the energy and matrix composition, might escape from the drum and even the calorimeter. Such losses of energy should be checked for and, if necessary, corrected for.
- It is not possible to shield the power generation. Once a steady state condition is reached, the whole power generated by the item under test is completely evacuated by the measurement chamber, regardless of the packaging of the item.
- Calorimetry, on the one hand, measures the summated heat deposition of all radioactive nuclides present. In that sense, none of the radioactive material can be missed, except for small amounts below the (sensitive) lower detection limit. On the other hand, calorimetry is not viable to discriminate various RN, unless prior knowledge from other means can be utilized.
- The measurement result is independent from material matrix composition and geometry (only assay time is affected). Thanks to this, it is not necessary to characterize the matrix in order to measure the radioactive sample.
- Without phase changes and chemical reactions, answer is bias free and not affected by self-attenuation effects. If, however, chemical reactions cannot be discarded from the pre-conditioning process of the waste package, non-radioactive heating must be investigated appropriately.
- The calibration of the instrument is standardized and can be verified.

On the other side, the calorimetric method is affected by the following limitations:

- The measurement accuracy can be degraded in case of materials with inhomogeneous isotopic composition, because of the uncertainty in the determination of the effective specific power. In general, the accuracy of the calorimetric measurement is related to the ability to determine the isotopic composition of the sample.
- The calorimetric assay features longer measurement time compared to other NDA techniques. Typical measurement times are in the order of several hours, even days for large samples with very low thermal power rates. Even the packaging of the source can still affect the measurement time, though not the accuracy, it.
- It usually requires very large equipment for accurate measurement results. Because of the relatively low power rates of nuclear samples and the large volume under test, usually the overall dimensions of standard equipment can be important and possibly limiting.
- If heat is produced by reactions others than nuclear, this cannot be discriminated by the calorimeter and this can bias the measurements.

Calorimetry is not likely a stand-alone NDA. It rather supplements gamma and neutron spectrometry, especially for declarable radionuclides (RN) with no or only too weak a gamma signals to be detected. Calorimetry is sensitive to all RN inside a waste drum, as all radiation emitted turns into heat, eventually (*i.e.* some radiation might also escape the drum and calorimeter). However, its stronghold is also its weakness as calorimetry detects all heat sources, exceeding its lower detection limit (LOD), of course, but does this without discriminating RN or isotope or location in the drum. Yet, another stronghold is its capability of measuring large volume compounds and, if need be, of heterogeneous content.

As the CHANCE project [3, 4] is focused on conditioned waste only, some pre-knowledge of the waste

composition and history may well be assumed, *f.i.* non-radioactive heat sources or sinks are generally negligible, and the results of preceding gamma and possibly neutron assay are known.

If representative sampling is possible and viable then, of course, the whole experimental tool-set of a full-range radio-chemical analysis (RCA) can be applied (*Figure 1*). In many cases of nuclear waste management, however, sampling and RCA is not (at first) possible.
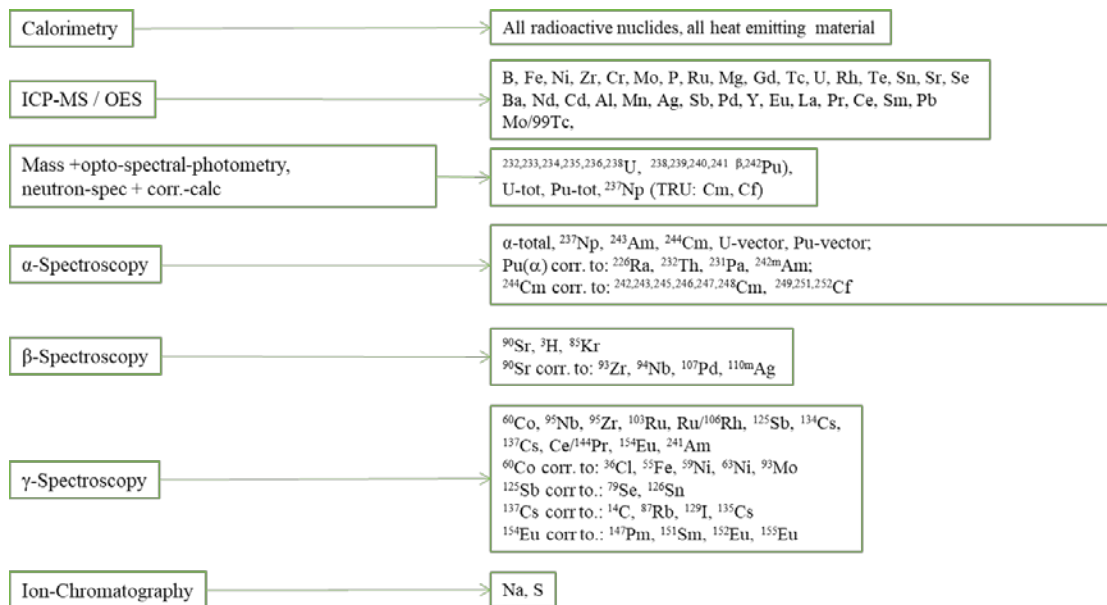
Calorimetry	→	All radioactive nuclides, all heat emitting material
ICP-MS / OES	→	B, Fe, Ni, Zr, Cr, Mo, P, Ru, Mg, Gd, Tc, U, Rh, Te, Sn, Sr, Se Ba, Nd, Cd, Al, Mn, Ag, Sb, Pd, Y, Eu, La, Pr, Ce, Sm, Pb Mo/99Tc,
Mass +opto-spectral-photometry, neutron-spec + corr.-calc	→	$^{232,233,234,235,236,238}U$, ^{238,239,240,241} β,^{242}Pu), U-tot, Pu-tot, ^{237}Np (TRU: Cm, Cf)
α-Spectroscopy	→	α-total, ^{237}Np, ^{243}Am, ^{244}Cm, U-vector, Pu-vector; Pu(α) corr. to: ^{226}Ra, ^{232}Th, ^{231}Pa, ^{242m}Am; ^{244}Cm corr. to: ^{242,243,245,246,247,248}Cm, ^{249,251,252}Cf
β-Spectroscopy	→	^{90}Sr, ^{3}H, ^{85}Kr ^{90}Sr corr. to: ^{93}Zr, ^{94}Nb, ^{107}Pd, ^{110m}Ag
γ-Spectroscopy	→	^{60}Co, ^{95}Nb, ^{95}Zr, ^{103}Ru, Ru/^{106}Rh, ^{125}Sb, ^{134}Cs, ^{137}Cs, Ce/^{144}Pr, ^{154}Eu, ^{241}Am ^{60}Co corr. to: ^{36}Cl, ^{55}Fe, ^{59}Ni, ^{63}Ni, ^{93}Mo ^{125}Sb corr to.: ^{79}Se, ^{126}Sn ^{137}Cs corr to.: ^{14}C, ^{87}Rb, ^{129}I, ^{135}Cs ^{154}Eu corr to.: ^{147}Pm, ^{151}Sm, ^{152}Eu, ^{155}Eu
Ion-Chromatography	→	Na, S

Figure 1: RCA methods for the determination of radionuclides and elements
(activities or masses per volume or waste compound)

So, essentially the experimental task of calorimetric NDA is either to verify or rule out the existence of additional RN that are not detectable by either gamma or neutron spectrometry. Thus, the task is determining the upper limit for the activity or mass of assumed beta- or alpha radiation heat source or the possibility of hidden / shielded gamma or neutron sources, such as a shielded Co-60 or Mo/Tc-99 or even a Cf-252 source that are used for medical purposes or as a reactor ignition source, eventually found in radwaste packages.

The ultimate objective for the characterization of RN is to meet the declaration requirements for the final disposal of the radioactive waste (RW) compound, which varies from country to country and for different repositories, too. However, there is a general tendency of the authorities to request more and more RN and chemo-toxic content and matrix material to be characterized and declared, despite the fact that metrological assay provides easy-to-measure (ETM) results for a hand-full of RN, only. The remaining RN are usually correlated to ETM-key-nuclides (Co-60, Sb-125, Cs-134, Cs-137, Eu-154), and the uncertainties, detection limits and maximum missed activities are thus correlated, too. *TABLE I* comprises the RNs that are to be declared for medium-active compacted and vitrified waste compounds to be disposed of in Germany. Whereas for high-level vitrified waste containers this RN-list required for Germany is older and contains significantly less declarable RN, though the same crucial key nuclides are determined (Co-60, Sb-125, Cs-134, Cs-137, Eu-154, *U-235*, U-238, *Pu-239,* Pu-241, Cm-244, Np-237, Am-241, Am-243). All others are derived from numerical correlations which are verified by the process performance and qualification.

	Radionuclide
Declarable RN	*H-3*, C-14, Cl-36, Ca-41, Mn-54, Fe-55, Ni-59, Ni-63, Co-58, *Co-60*, Se-79, Kr-85, *Sr/Y-90*, Zr-93, Zr-95, Nb-94, Mo-93, Tc-99, Ru-103, *Ru/Rh-106*, Pd-107, Ag-110m, Sb-125, Sn-126, I-129 *Cs-134*, Cs-135, *Cs-137*, Ce/Pr-144, Pm-147, Sm-151, Eu-152, Eu-154, Eu-155, Ra-226, Th-232, Pa-231, U-232, U-233, U-234, U-235, U-236, U-238, Np-237, *Pu-238*, Pu-239, Pu-240, Pu-241, Pu-242, Am-241, Am-242m, *Am-243*, Cm-242, Cm-243, *Cm-244*, Cm-245, Cm-246, Cm-247, Cm-248, Cf-249, Cf-251, Cf-252
Additionally declarable	U_{total} , Pu_{total} , α_{total} , β_{total}
Additionally declarable RN (repository-dependent from long-term safety assessment)	Ag-108m, Ac-227, Th-229, Th-239, Pu-243, Pu-244

TABLE I: Declarable RN in compacted or vitrified ILW (for Germany) [12].
The "underlined" RNs are β-only emitters without significant heat deposition,
"bold, italic" RN deposit measurable heat.

The RN list of *TABLE I* is considered a token for the declaration task, and to which degree calorimetry is expected to add value to the results. In particular historical and large volume RW-compounds calorimetry is expected a stronghold. A number of declarable RN amongst the listed (*TABLE I*) ones cannot be measured easily by gamma- or neutron-spectrometry, namely the RNs (H-3, Sr/Y-90, Ru/Rh-106, Pu-238, Am-243, Cm-244) deposit a measurable radiation heat (*cf. TABLE II*) and are difficult to detect by other NDA surveys. Moreover, sealed radioactive sources deposit their radiation heat while the shielding prevents gamma radiation to emerge. These are the candidates to be addressed using calorimetry, and biased knowledge from the preconditioning process helps to rule out potential contribution from other heat sources.

Isotope	Specific power [mW/g]	Transition / branching ratio	Energy [keV]
H-3	**324**	**β / 100%**	**5.7**
(C-14)	1.3	β / 100%	49,5
(Cl-36)	0.06	β / 100%	298
Co-60	*649*	*β / 4% - γ / 96%*	*97 (β) / 2504 (γ)*
(Sr)/Y-90	**3 E6**	**β / 100%**	**933**
(Mo/Tc-90)	0.006	β / 100%	55,2
Ru/Rh-106	**30 E9**	**β / 87% - γ / 13%**	**206 (β) / 1413 (γ)**
Cs-134	*1256*	*β / 10% - γ / 90%*	*164 (β) / 1554 (γ)*
Cs-137	*125*	*β / 29% - γ / 71%*	*244 (β) / 597 (γ)*
Pu-238	**568**	**α / 100%**	**5579 (α) / 1.9 (γ)**
(Pu-241)	3.3	α / 2% - β / 98%	0.12 (α) / 5.2 (β)
Am-241	**115**	**α / 99%**	**5581 (α)**
Cm-244	**2829**	**α / 100%**	**5892 (α)**

TABLE II: Specific power and branching ratio for some selected radionuclides [13].
For the bold ones, calorimetry appears a viable method; the italic ones are better
measured by gamma-spectroscopy; the ones in brackets are likely to remain
undetected by calorimetry. For β emitters, the energy indicates the mean β energy.

The measurable heat flux [W] or thermal power W_{RN} [W] deposited is the simple product of the specific thermal radiation power deposition P_{RN} [W/g] multiplied with the mass m_{RN} of the radionuclide:

$$W = m\,P \qquad \text{or} \qquad W_j = \sum_i m_{ij} P_{ij} \qquad (1)$$

Where j denotes the different radionuclides RN_j, i runs over the isotopes RN_j(i) and m_i denotes the mass fractions, respectively. P_i is their associated specific power. W is the experimentally accessible variable.

Uncertainty considerations derive directly from equation (1), statistical considerations, uncertainty propagation and from the measurable variables associated with the specific experimental set-up. The nuclear characterization task asks for m_{ij}, thus resolving equation (1) for m_{ij} which requires additional information about i and j, i.e. the radionuclide m_j and in many cases the nuclide vector m_i, as well. Calculating the heat-load resulting from gamma- and neutron measurements often matches the calorimetric results unless significant heat sources are hidden inside the compound. This can be detected but the heating RN(s) cannot be identified. However, solving equation 1 for the additional unknown heat source determines an upper limit of the spurious mass or activity associated with a specific RN, and considering the associated uncertainty would establish an upper limit or maximum missed activity or mass (MDM), respectively.

MCNP CALORIMETER MODELLING

Calorimetry is not bias-free. Source position, material density distribution, chemical reactions, phase changes and also radiation leakage can influence the final result. In order to evaluate how the leakage impacts on the result and how the radiation behaves within the volume of the calorimeter (i.e. how the energy is deposited inside the system and to estimate the amount of escaping flux) Monte Carlo modelling of the KEP-LVC calorimeter (*Figure 2*) was realized, using the MCNP6 code and ENDFB-7.1 cross sections library [13].

Based on the conceptual KEPIC (KEP Innovation Center) design (*Figure 2*), the numerical model was simplified for the relevant parts and for particle transport simulations.
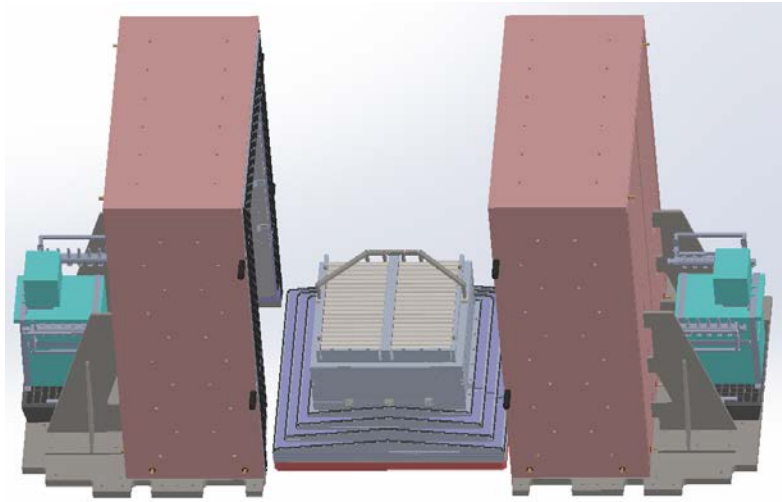
Figure 2: 3D view of the CHANCE Calorimeter

The MCNP model presented in *Figure 3* consists of different layers: at the center is a sand [14] filled drum and an assembly with radioactive material. The next layer is the octagon-shaped structure with the heat flux detectors on each wall, inside the measurement chamber filled with air. Then, there are in total four homogenization layers alternating with insulation layers. Below the measurement chamber is a reference chamber (or ghost chamber) with a phantom aluminum block that compensates the influence of the ambient environment (*e.g.* temperature changes). The outer aluminum layer (or cold plate) is kept at a constant temperature to decouple the system from outside influence.
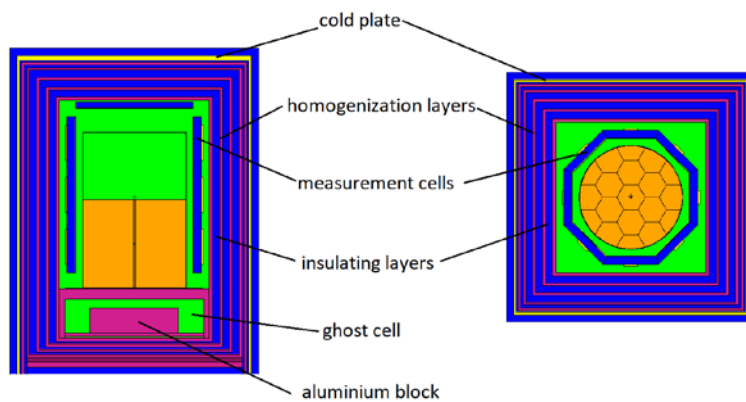
Figure 3: MCNP geometry 2D views. Left: xz plan view. Right: xy plan view.

Two kinds of generic radiation sources were used in the modelling. One source, hereafter called the "most conservative" source, was filled up to 50cm with an assembly of pins with containers containing a generic heat source mocking radioactive material (*Figure 4*); the remaining part was filled with air. The space between the pins was filled with sand [14]. In this study, the most conservative source was limited to only one pin in the center of the assembly with only one container in the middle of the pin. In this scenario emerging particles have the longest possible pathway to leave the system.
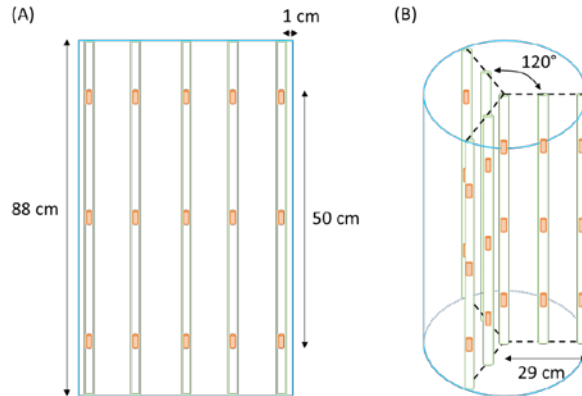

Figure 4: Possible source positions considered here, based on the geometry provided by [15] .

A second generic source, hereafter called the "homogeneous" source, was a 50cm sand [14] filled drum and air on top. The particle starting points were sampled inside the whole section filled with sand. The amount of escaping radiation is of course higher in this case, as the particles may appear nearby the wall of the drum. *Figure 5* illustrates the difference between the both source configurations.
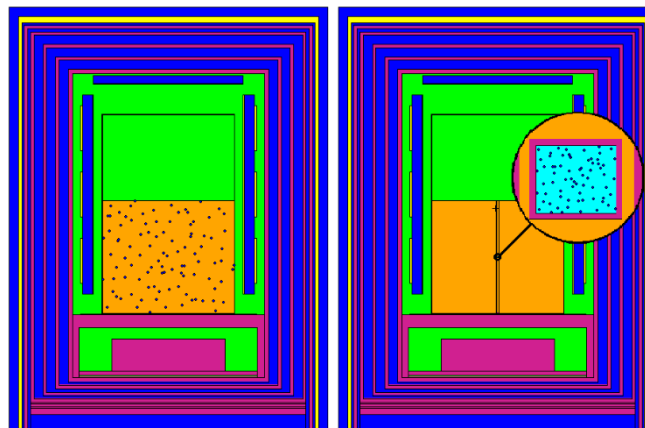

Figure 5 : Homogeneous (left) and most conservative (right) source configurations.

To calculate the gamma and neutron emission rates the numerical model comprises:

- **Compositions**: The same matrix and drum compositions were used here, but additionally, sand was also considered, as it might be a practical alternative to a cement-based matrix to use with existing mock-up drums. For the plutonium, we used a typical reactor-grade composition [14].

- **Sources**: For the gamma source, the same peaks were considered. For the neutron source, a spontaneous fission source was considered instead of explicit specification of the energy distribution, but this leads to very comparable results.
- **Particle flux**: The MCNP type 1 tally was used to get a direct estimate of the number of particles crossing the outer surface of the drum.

Only the plutonium sources are considered currently in the models. The skeleton that holds them in place is not taken into account.

RESULTS; GAMMA and NEUTRON FLUX DISTRIBUTION

Using a tally 4 with the mesh option the mean gamma flux in each cell of a defined grid (mesh option) yields the number of particles per cm^2, per source particle. The flux was checked along the x axis at z = 74 cm (at height of the source position) and y = 0 and along the z axis at x and y equal to 0. A generic mono-energetic gamma source of 1.0MeV was used; the results shown in Figure 6 a) and b) along the z-axis and x-axis for the most conservative and homogeneous source models, respectively.
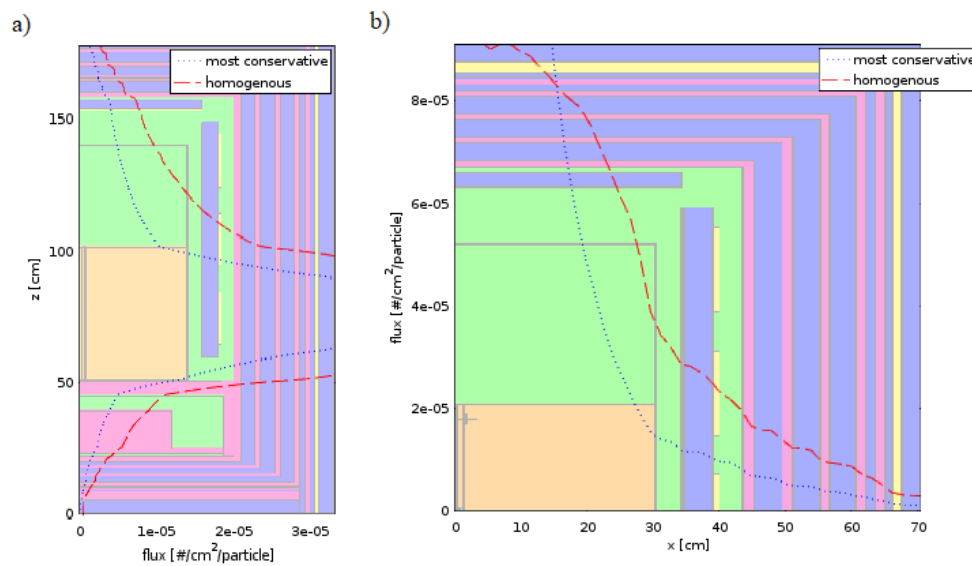

Figure 6: 1 MeV Gamma particle flux, most conservative source and homogeneous source – profile at (x;y) = (0;74)cm (a, left) and (y;z) = (0;74)cm (b, right).

The flux decreases rapidly inside the drum and a bit less within the walls. A certain amount of the radiation energy is not deposited inside the system (up to $10^{-5}cm^{-2}$ in case of the most conservative source and $10^{-3}cm^{-2}$ in case of the homogeneous one).

Figure 6 a) shows the gamma particle flux along the z-axis for the 1 MeV homogeneous and most conservative source models. Figure 7 a) shows the gamma particle flux along the z-axis for the homogeneous source models at 0.1MeV, 1MeV and 5MeV energy source. Obviously, the radiation penetrates the aluminum block and ghost cell (reference part). Heating of this part can cause an additional

bias. This phenomenon is visible for both the most conservative and homogeneous source and radiation energy of 1MeV and 5MeV.
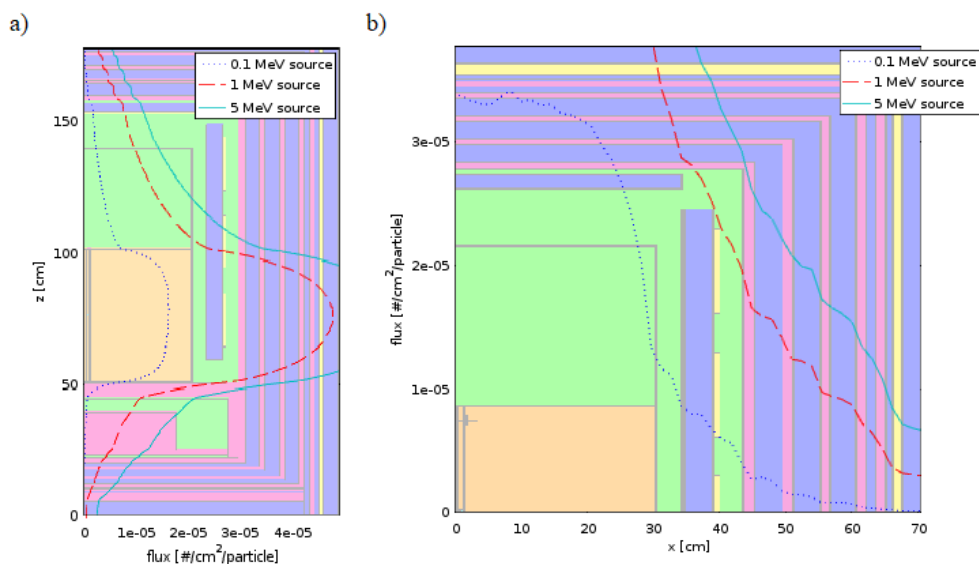

Figure 7, Gamma particle flux for 0.1MeV, 1 MeV and 5MeV, homogeneous source – profile at (x;y) = (0;74)cm (a, left) and (y;z) = (0;74)cm (b, right).

In analogy with the gamma source simulations, a generic mono-energetic neutron source of 0.1-5 MeV was used, also in the homogeneous and most conservative set-ups. The obtained neutron flux distribution along the x- and z-axis, respectively, are qualitatively very similar to the gamma distributions (*Figure 6, Figure 7*) except for different scaling of the absolute numbers. Again, tally 4 was used to determine the particle fluxes, and for neutrons the radiation flux escaping the calorimeter was around $1 \cdot 10^{-5} \text{cm}^{-2}$ in case of the most conservative source and $3 \cdot 10^{-5} \text{cm}^{-2}$ in case of the homogeneous source.

Not surprisingly, a significant and similar part of the neutron flux penetrates the reference elements just like gammas, which causes additional bias.

ENERGY DEPOSITION from a Co-60 SOURCE

Apart from the flux behavior, the energy deposition in each part of the calorimeter was calculated using tally 6 which it determines energy deposition per one gram of material in a cell. We used a generic Co-60 source emitting two gamma-lines at 1.332MeV and 1.173MeV at 99.88% branching ratio. The data were normalized to the equivalent of 1g of Co-60 source strength.

The results for both, the homogeneous and the most conservative source models are presented in *TABLE III*. The heat depositions in the layers were divided into three components: energy that was detected by the measurement elements (bold), energy that will reduce the final result (italic) and parts with negligible influence on the power measurement (all other).

Layer	Homogeneous source			Most conservative source		
	energy [MeV/g]*	power [mW/g]**	Energy deposition [%]	energy [MeV/g]*	power [mW/g]**	Energy deposition [%]
drum	**1.57E+00**	**1.05E+04**	**72.27**	**2.18E+00**	**1.46E+04**	**87.24**
thermal block	1.70E-01	1.14E+03	6.77	5.85E-02	3.93E+02	2.35
homogenization layer 1	1.00E-01	6.71E+02	3.99	3.47E-02	2.33E+02	1.39
homogenization layer 2	8.15E-02	5.47E+02	3.25	2.83E-02	1.90E+02	1.13
homogenization layer 3	6.63E-02	4.45E+02	2.65	2.30E-02	1.54E+02	0.92
homogenization layer 4	5.32E-02	3.57E+02	2.12	1.83E-02	1.23E+02	0.73
cold plate	4.65E-02	3.12E+02	1.86	1.61E-02	1.08E+02	0.64
measurement plates	**4.55E-02**	**3.05E+02**	**1.82**	**1.45E-02**	**9.74E+01**	**0.58**
aluminum block	*1.29E-02*	*8.68E+01*	*0.52*	*5.75E-03*	*3.86E+01*	*0.23*
reference plates	*1.09E-02*	*7.32E+01*	*0.44*	*3.75E-03*	*2.51E+01*	*0.15*
bottom measure-ment plate	1.03E-02	6.89E+01	0.41	3.69E-03	2.48E+01	0.15
measurement cells	**1.13E-03**	**7.61E+00**	**0.05**	**3.50E-04**	**2.35E+00**	**0.01**
insulation layer 1	1.01E-03	6.78E+00	0.04	3.38E-04	2.27E+00	0.01
insulation layer 2	8.23E-04	5.53E+00	0.03	2.74E-04	1.84E+00	0.01
insulation layer 3	6.65E-04	4.46E+00	0.03	2.23E-04	1.50E+00	0.01
measurement chamber	**4.94E-04**	**3.32E+00**	**0.02**	**1.54E-04**	**1.04E+00**	**0.01**
insulation layer 6	3.31E-04	2.22E+00	0.01	1.10E-04	7.38E-01	0.00
insulation layer 4	2.06E-04	1.38E+00	0.01	6.89E-05	4.62E-01	0.00
insulation layer 5	1.10E-04	7.40E-01	0.00	3.68E-05	2.47E-01	0.00
ghost chamber	*6.20E-05*	*4.16E-01*	*0.00*	*2.08E-05*	*1.40E-01*	*0.00*
sum total	2.17E+00	1.46E+04	86.59	2.38E+00	1.60E+04	95.59
sum detected	1.59E+00	1.07E+04	73.19	2.18E+00	1.46E+04	87.46

TABLE III: Energy deposition of a Co-60 source in the calorimeter. energy that was detected by the measurement elements (bold), energy that will reduce the final result (italic) and parts with negligible influence on the power measurement (all other)

* energy deposited in one gram of the material in the layer

**calculated power of one gram of the radioactive material

The relative error was <1% for each part (cell) of the calorimeter. One can see that about 4% of the radiation escaped the calorimeter and 87% would be detected in case of the most conservative source configuration. About 13% of the radiation escaped the system and ~73% would be detected in case of homogeneous source.

SUMMARY and CONCLUSION

Depending on the source configuration and particle types, between 4% - ~13% of the energy escaped the system and 73% - 87% was detected. The amount of deposited energy in the reference element was no bigger than 1.5%. This deposited energy is not measured by the Peltier elements, and the final result would be reduced by this value. The maximum bias caused by this phenomenon is <3%. The percentage of the total energy deposited depends on the source energy, i.e. low-energy emitters are less biased than high-energy ones.

MCNP simulations were performed for generic source and matrix compositions to quantify the percentage of particles (mainly gamma and neutrons) leaving the waste drum. While escaping radiation can be largely hampered with these matrices, the heat flux is unaffected, thus demonstrating the usefulness and complementarity of calorimetry in these cases and in general.

MCNP simulations of the calorimeter suggest that the uncertainty related to the energy deposition, based on uncertainty on the distribution of activities within a drum, is smaller than the two orders of magnitude. Therefore, we also demonstrated the usefulness of calorimetry in cases with unknown distribution of activities within drum.

REFERENCES

[1] D.S. Bracken, C.R. Rudy, Principles and applications of calorimetric assay, LA-UR-07-5226
[2] D.S. Bracken, R.S. Biddle et. al., Application Guide to Safeguards Calorimetry, LA-13867-M, January 2002
[3] D. Ricard, S., Plumeri, L. Boucher, A. Rizzo, H. Tietze-Jaensch, C. Mathonat, C. Bruggeman, J. Velthuis, L Thompson, G. Genoud, C. Bucur, D. Kikola, G. Zakrzewska-Koltuniewicz, (2018). The CHANCE project "Characterization of conditioned nuclear waste for its safe disposal in Europe". DEM 2018 - Dismantling Challenges: Industrial Reality, Prospects and Feedback Experience, France, Avignon – 2018, October 22 – 24
[4] CHANCE 2020 : http://chance-h2020.eu
[5] CHANCE delivery report D3.1 published on http://chance-h2020.eu [4]
    W. R. Kubinski, MSc. Thesis, Faculty of Physics, Warsaw Univ. of Technology, Sep. 2018
[6] J. Ph. Houriet, Monitoring des déchets radioactifs: Mise à jour 1984, Rapport Technique 84-10. - Würenlingen : Institut fédéral de recherches en matière de réacteurs.
[7] S.- T. Hsue et al. Guide to Nondestructive Assay Standards: Preparation Criteria, Availability, and Practical Considerations, LA-13340-MS report, Los Alamos National Laboratory, 1997.
[8] J. L. Dufour , B. Autrusson and P. Funk, Waste Drums Measurements.: Scientific documentation from the Institute de Radioprotection et de Sûreté Nucléaire-Radioactive Material Security Department (IRSN).
[9] P. Funk P. and B. Autrusson, Characterisation of the Content of a Radioactive Waste Drum: Example of Techniques Used in France for Plutonium Measurement. - : Scientific documentation from the Institute de Radioprotection et de Sûreté Nucléaire-Radioactive Material Security Department.
[10] IAEA Strategy and Methodology for Radioactive Waste Characterization, IAEA report IAEA-TECDOC-1537 - Vienna : 2007.
[11] Rackham J., Weber A.L. and Chard P. Performance Values for Non-Destructive Assay (NDA) Technique Applied to Wastes: Evaluation by the ESARDA NDA Working Group, ESARDA Bulletin Bulletin. - 2012. - Vol. 48. - pp. 25-78.

[12] K. Kugel and K. Möller, Endlagerungsbedingungen Konrad - 2017. - https://www.endlager-konrad.de/SharedDocs/Downloads/Konrad/DE/fachunterlagen/endlagerungsbedingungen_konrad.pdf?__blob=publicationFile&v=7.

[13] NEA OECD-NEA - 2018. - www.oecd-nea.org/janisweb/search/endf.

[14] US Department of HomeLand Security: Compendium of Material composition Data for Radiation Transport Modeling, PIET-43741-TM-963, PNNL-15870 Rev. 1, US Department of HomeLand Security, 2011.

[15] M. Bickel [et al.] New standards for the measurements of plutonium in radwaste. Proceedings of the symposium on safeguards and nuclear material management, 21st Annual meeting, ESARDA. - 1999. - pp. 4-6.

[16] Framatome ANP MOX Fuel Design Report. BAW-10238 (NP) Revision 0. 43-10238NP-00. - 2002.

[17] A. R. Massih, Models for MOX fuel behaviour. SKI Report 2006:10. ISSN 1104-1374. iRSN SKI-R/06/10-SE. - 2006.

[18] K. Konno and T. Hirosawa, Melting temperature of simulated high-burnup mixed oxide fuels for fast reactors Journal of nuclear science and technology. - 1999. - Vol. 36(7). - pp. 596-604.